Experimental Investigation into the Flexural Behavior of Hollow, Full, and Intermittently Stiffened (bamboo-like) Glulam Beams from Larch Wood

Xiaofeng Zhang,[a] Lisheng Luo,[b] Haiyan Fu,[a] Youfu Sun,[a,*] and Xiran Hui [a]

Bamboo-like glulam beams with hollow section units and intermittent internal reinforcement pieces were produced with small-diameter larch-wood pieces and one-component polyurethane. To better understand the design reliability, the failure mode, ultimate bearing capacity, and application potential were evaluated. Three types of beams (solid glulam, hollow glulam, and bamboo-like rectangular glulam beams) were compared and analyzed in this work. Stiffener pieces glued inside the bamboo-like beam were found to increase the bearing capacity and improve the failure mode relative to the hollow glulam beam. Comparison of the hollow section with a similar outside diameter showed that the ultimate bearing capacity increased by approximately 12.3% when the spacing between the stiffeners was 270 mm, and the ultimate bearing capacity increased by approximately 18.0% when the spacing between the stiffeners was 135 mm. Compared with the solid timber beams, wood consumption was reduced by 26.4% and 25.7% for the hollow and bamboo-like glulam beams, respectively. Also, a parameter analysis of the reasonable spacing and thickness of the stiffener was proposed by the finite element method.

Keywords: Glulam beam; Bamboo-like; Stiffener; Bearing capacity

Contact information: a: Department of Wooden Structure Construction, College of Materials Science and Engineering, Nanjing Forestry University, Nanjing 210037, China; b: College of Civil Engineering and Architecture, Hainan University, Haikou 570228,China;
** Corresponding author: yfsun@njfu.edu.cn*

INTRODUCTION

Glued laminated timber (glulam), an engineered wood product, was developed during the 19th century in Europe and has been used in engineering fields because of its high strength to weight ratio, as well as its aesthetic properties, easy processing, strength, and dimensional stability (Anshari *et al.* 2010).

There are many advantages in common between the gluing and splicing processes. The splicing process is the method of making beams using traditional Chinese craftsmanship. It refers to the crushing of complex shapes with small pieces or simple shapes to replace big-diameter timber with small-diameter timber. The split beam has a long history, and it has been seen in buildings from the Tang Dynasty (Zhao *et al.* 2014).

Currently, research is underway on steel-timber composite beams and timber-concrete composite beams to determine their process and mechanical properties (Ghavami 1995; Capozucca 1998; Eisenhut *et al.* 2016; Bradford *et al.* 2017; Keipour *et al.* 2018). According to the status quo of forestry resources in China and inspired by bamboo, a new type glulam beam with a hollow section unit has been proposed, which is manufactured with small-diameter larch (*Larix olgensis* Henry) and one-component polyurethane. It is

based on a hollow glulam beam, within which internal pieces called "stiffeners" are adhered at intervals to increase its ultimate bearing capacity. The spacing of the stiffeners can be adjusted according to load requirements and their own thickness. Because the structure has similarities with bamboo, except that it has a rectangular cross-section, it will be defined here as a bamboo-like glulam beam. Also, the section has potential to be used in various structures and applications, such as in building columns or as an alternative to steel street lighting and traffic light poles (Gilbert *et al.* 2014). Furthermore, this beam with a hollow section unit has developed a market for low-value, small-diameter timber in many countries. This is a reasonable measure to save forest resources and contribute to sustainable environmental development.

To use these novel sections in structural applications, experimental tests must be done to confirm the structural behavior and failure modes, therefore ensuring reliable design properties (Gilbert *et al.* 2014, 2018). According to the literature, various hollow section components have been proposed to utilize small-diameter logs or replace solid timber members in the building structure market. Hollow octagonal utility poles are manufactured with composite wood flake panels, and the poles are tapered with the wall thickness decreasing as the height decreases. Additionally, the feasibility, design strength, and cost have been analyzed. It has been found that the proposed poles can be cost-competitive in the industry (Adams *et al.* 1979). Since 1994, Kyoto University has been working on composite structures and found that low quality logs have a remarkable influence on the strength of the product when used for veneer tapes and between butt-jointed veneers (Hara *et al.* 1994; Sasaki and Kawai 1994). Sasaki and Kawai (1994) proposed a hollow cylindrical laminated veneer lumber (LVL); a series of studies have been carried out, and they have indicated that this LVL exhibits a high strength and can be used in construction. Zhang *et al.* (1997) studied a type of hollow bamboo-wood composite slab (consisting of bamboo-based panels and Masson pine strips) and explored the effect of the hollow ratio of this plate on the mechanical properties. The test results showed that the section can be designed and the hollow ratio has no remarkable effect on the stiffness, but has a noticeable effect on the strength (Zhang *et al.* 1997). Harries *et al.* (2000) performed axial and bending tests on hollow composite columns. When compared with solid sections, the hollow sections had advantages in the carrying capacity when its diameter was greater than 127 mm × 127 mm (Harries *et al.* 2000). Wei (2005) studied cylindrical veneer lumber, which is a spirally wound structure in which the veneers are processed into a staggered laminate. As a result, a decrease in the elastic modulus is suppressed. When cylindrical LVL is produced, the elastic modulus of the laminated material is reduced to a small extent in the range of an angle of no more than 10°, and glass fiber can enhance the dimensional stability of cylindrical LVL. Cylindrical LVL has good mechanical properties, excellent engineering properties, and can be used in construction and other fields (Wei 2005). Cai (2014) proposed a single-plate laminated hollow column. It was found that local stress and strain concentrate at the bottom during the stress process. According to the conclusion of an ANSYS simulation by Cai (2014), it is necessary to strengthen the end of the hollow column to ensure its bearing capacity in practical applications. Hollow veneer-based composite utility poles are manufactured from a hard plantation of thinned trees to find a solution and change the current shortage of traditional solid utility poles in Australia. Gilbert *et al.* (2014) showed that the proposed cross-section will have an external diameter approximately 1.2 times greater than the former and would be approximately two times lighter. Hartig *et al.* (2016) produced a molded wooden tube made of beech with a height of 3 m, diameter of 0.32 m, and wall thickness of 0.02 m.

Experimental and theoretical investigations showed that the wood molding process did not impair the structure of the material; in contrast, it increased the stiffness (Hartig *et al.* 2016). Shang *et al.* (2018) studied the bending behavior of a hollow Xingan larch (*L. dahurica*) glulam beam. Additionally, they studied the influence of the wall thickness and hollow ratio on the flexural capacity and stiffness of the hollow beam (Shang *et al.* 2018). Aicher and Tapia (2018) used a novel composite of softwood glulam with internal beech LVL layers in their study. The experimental and theoretical investigations showed that the composite was damage-tolerant and excelled at non-brittle fracture. The mechanical properties of the novel glue-laminated timber-laminated veneer lumber (GLT-LVL) composite beam structure were superior, especially its suitability to accommodate large holes (Aicher and Tapia 2018).

This work introduced experimental materials, specimen design, and experimental methods for production of bamboo-like glulam beams. The performance of the studied sections was compared with that of solid and hollow glulam beams. Also, the ultimate bearing capacity and failure modes of the three different sections were analyzed and discussed. Finally, the reasonable spacing and thickness of the stiffeners were determined by the finite element method.

EXPERIMENTAL

Materials

The wood used was Northeast China larch (*L. olgensis* Henry), with diameters that ranged from 50 mm to 120 mm. This larch is a type of a domestic, fast-growing tree and was supplied by Xingyuan Wood Industry Co., Ltd. in Nanjing, China. The mechanical properties of larch can meet the production requirements for glulam (Wang *et al.* 2008). The dimensions were 4000 mm × 80 mm × 80 mm, and the grade was II_a, according to the visual stress grading method (GB 50005 2003). The properties of the materials were obtained *via* testing by referring to ASTM D4761-13 (2013). The final moisture content of the wood was 12.9% and the density was 0.63 g/cm^3. The compressive strength parallel to the grain was 43.0 MPa, the tensile strength parallel to the grain was 71.8 MPa, the ultimate compression strain parallel to grain was 5040 με, and the ultimate tensile strain parallel to the grain was 5120 με. Additionally, the bending modulus was 14,000 MPa.

A single-component polyurethane was used, and was supplied by Shanghai Donghe Adhesive Co., Ltd (DH 106, Shanghai, China).

Specimen Design

All of the test specimens were manufactured in a laboratory at Nanjing Forestry University (Nanjing, China), with an ambient temperature of approximately 23 °C to 25 °C and a humidity of approximately 53% to 56%. The test material was naturally dried to a moisture content of less than 13%, and was then subjected to sawing, planing, sizing, cold pressing, and curing processes.

In total, 12 timber beams over four groups were tested to examine the bending performance. All of the specimens had the same external section size. The length along the wood grain direction was 1800 mm, the height was 88 mm, and the width was 56 mm.

Table 1. Dimensions of the Specimens

No.	ZJA	ZJB	ZJC	ZJD
Web Thickness (mm)	—	16	16	16
Slab Thickness (mm)	—	16	16	16
Base Plate Thickness (mm)	—	16	16	16
Stiffener Width (mm)	—	—	24	24
Stiffener Thickness (mm)	—	—	14	14
Number of Stiffeners	—	—	7	13
Internal Height (mm)	—	56	56	56
Internal Width (mm)	—	24	24	24
φ (%)	—	27.3	26.4	25.7

φ – Hollowness ratio, the percentage of the hollow volume *vs.* the apparent volume of the glulam beam

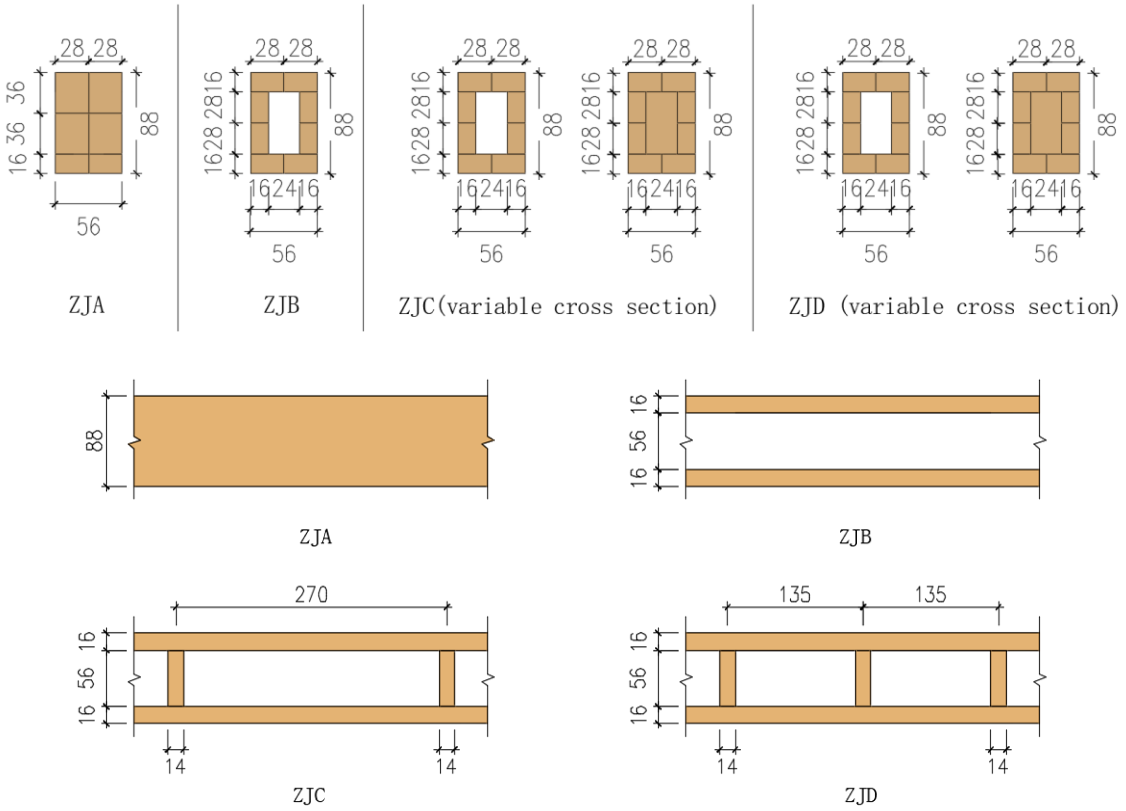

Fig. 1. Cross sections (mm) of the specimens

The specimens included three solid glulam beams labeled ZJA1 to ZJA3, three hollow glulam beams labeled ZJB1 to ZJB3, three bamboo-like (with intermitted insertion of stiffener pieces) glulam beams with a stiffener spacing of 270 mm labeled ZJC1 to ZJC3, and three bamboo-like glulam beams with a stiffener spacing of 135 mm labeled ZJD1 to ZJD3. According to ASTM D198-15 (2015) and CECS 254 (2009), the section hollow ratio of the hollow and bamboo-like glulam wood beams was defined. The specific size parameters of the specimens are shown in Table 1.

Experimental Methods

The tests were performed in the Wood Structure Laboratory of Nanjing Forestry University with an ambient temperature of approximately 22 °C to 25 °C and humidity of approximately 52% to 57%.

Figures 2 and 3 show the loading test method. For each test, the beam was positioned horizontally on the loading device in the direction of the grain. Five strain gauges were arranged equidistantly along the height direction of the beam span (BX120-20AA, Heshan District Guangce Electronics Co. Ltd., Yiyang, China). The length direction of the strain gauge was consistent with that of the wood along the grain direction, and the gauges were numbered 1 to 5 from top to bottom. A thimble displacement sensor (CPD-25, Shimadzu International Trading (Shanghai) Co. Ltd., Shanghai, China) was set at two fulcrum points at the end of the beam. There was an additional displacement sensor (YHD-100, Jiangsu Liyang Instrument Factory, Changzhou, China) at the mid-span on the bottom, which measured the settlement of the beam end supports and the change of the mid-span deflection, with an accuracy of 0.001 mm.

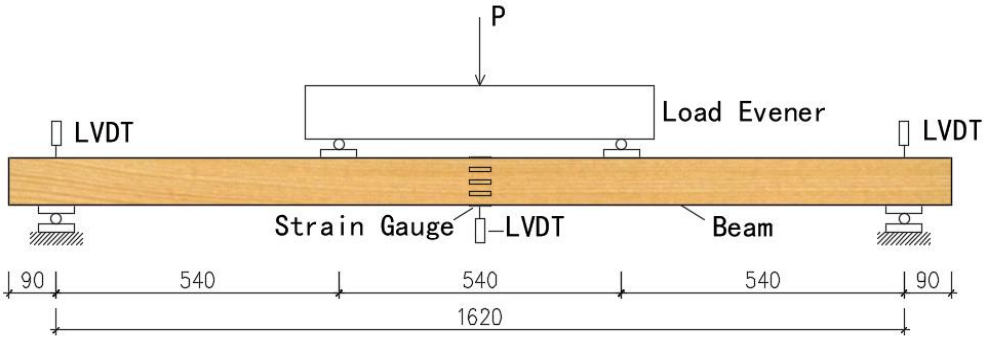

Fig. 2. Loading device and test point arrangement, LVDT- Displacement measurement (mm)

(a) **(b)**

Fig. 3. Loading process of the test (a) before and (b) after loading

The test was done using an electronic universal testing machine (UTM5105, Shenzhen Sansi Vertical and Horizontal Technology Co. Ltd., Shenzhen, China) with a maximum load of 100 kN, and the measured data was collected by a static data acquisition instrument (TDS-530, Tokyo Measuring Instruments Lab., Tokyo, Japan). According to GB/T 50329 (2012), a support steel pad was placed on the lower surface of the specimen to prevent lateral compression of the wooden beam. The width of the support steel backing plate was larger than the width of the beam section, the length was 80 mm, and the thickness was 10 mm.

A four-point bending experiment was developed according to ASTM D198-15 (2015). Before formal loading, the F_0 and F_1 values of each specimen were estimated. The F_0 value was taken as 0.5 kN to ensure that the loading plate and support pad were in close contact with the wooden beam, and the F_1 value was taken as 5 kN, which was less than the proportional limit force value. After loading started (the force control mode was adopted at the beginning), the load started at the F_0 value and increased to the F_1 value, then the load was unloaded to the F_0 value, and the cycle was repeated five times in accordance with the loading mode to calculate the elastic modulus of the beam.

After the 5th cycle the test was then conducted monotonically with a loading rate of 2 mm/min until complete failure .

The work performance of the glulam beam was numerically simulated and verified by Workbench 15.0 with ANSYS finite element software (ANSYS Company, Pittsburgh, Carlisle, PA, USA).

Main Results of Testing

The specific test results of all 12 glulam beam specimens are shown in Table 2. For the flexural glulam beams, the apparent elastic modulus (MOE) and equivalent flexural strength (MOR) were converted according to the test results. The conversion formula was as follows,

$$\mathrm{MOE} = \frac{a\Delta P}{48I\Delta\omega}(3l^2 - 4a^2) \quad (1)$$

$$\mathrm{MOR} = \frac{P_u a}{W} \quad (2)$$

where a is the distance from the loading point to the support (mm), ΔP is the load increment of the elastic stage (N), l is the calculated span of the beam specimen (mm), I is the moment of inertia of the beam section, W is the section modulus of the beam section, and P_u is the ultimate load (kN).

RESULTS AND DISCUSSION

Failure Mode Analysis

There were three typical failure modes in the specimens, and the specific failure modes are shown in Figure 4. First was brittle tensile failure. The glulam beam showed obvious plastic deformation in the late stage of loading, and the stiffness of the beam decreased. As the load continued to increase, a crack appeared in the beam span near the bottom plate, which was accompanied by a tearing sound from the wood fiber. The crack continued to increase, the layered tear at the bottom of the glulam beam was destroyed, and

the bearing capacity decreased rapidly. After unloading, the deflection of the wooden beam was restored to the initial stage, but there was partial plastic deformation. The second failure mode was web shear failure. In the ZJB and ZJC groups, the hollow glulam beam webs were subjected to large shear stress. This led to the first crack at the loading point to the bearing area of the hollow glulam beam. The crack developed obliquely until shear failure occurred. Because of insufficient development of plastic deformation during shear failure, the equivalent bending strength (MOR) of the ZJB group was smaller than that of the other groups. Also, it was evident that the stiffeners improved the failure mode of the glulam beams. The third failure was tensile ductility destruction. In the ZJC and ZJD specimen groups, the compressive side of the wood fibers first reached the yield strength during the loading process and the stress remained unchanged. The strain increased and the beam was plasticized, which was accompanied by the sound of the internal wood fibers breaking. Deformation occurred until the tensile side of the wood fiber reached the ultimate tensile strain and exhibited ductility.

It was found that stiffeners improved the failure mode of the hollow timber beams and increased their ultimate bearing capacity and bending strength.

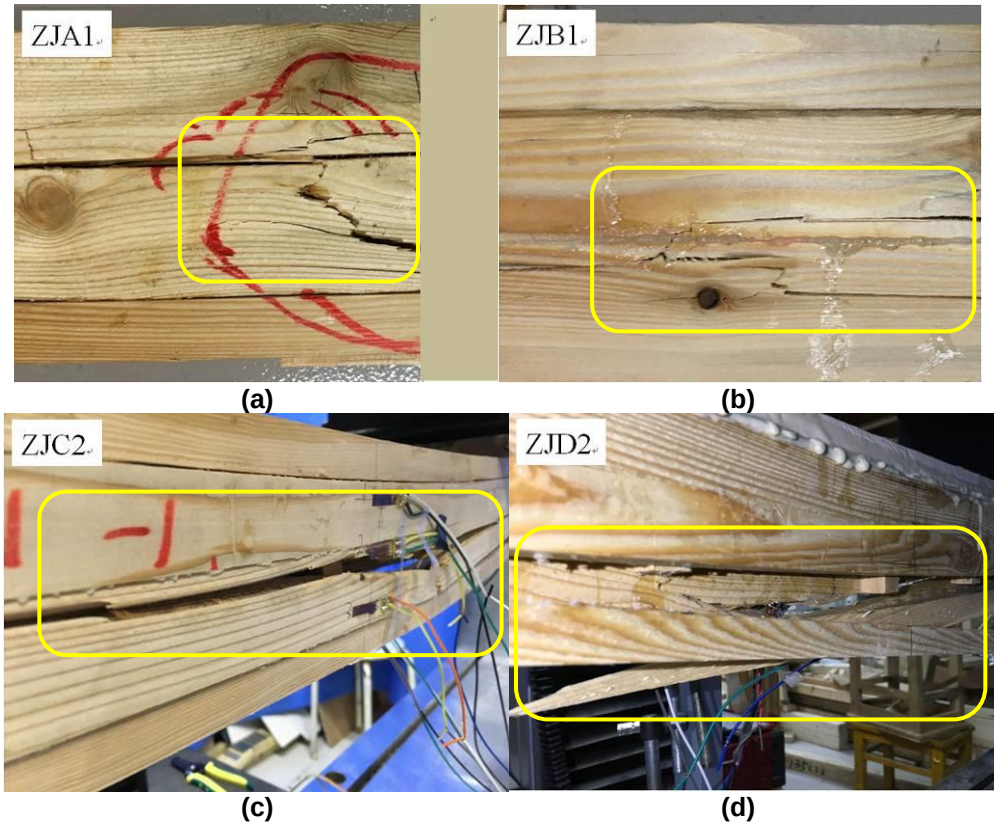

Fig. 4. Failure mode of the specimens: (a) ZJA1, (b) ZJB1, (c) ZJC2, and (d) ZJD2

All of the specimens showed elastic characteristics during the initial stage of loading, and the force-controlled cyclic loading was performed in the elastic stage. Because of the presence of a small amount of knots in the glulam beam, the bending stiffness of the beam was reduced and the MOE of the glulam beam was reduced. This resulted in the MOE of the glulam beam in Table 2 being less than the MOE obtained from the experimental material. Compared with the hollow glulam beam, the average ultimate

bearing capacity of group C increased by approximately 12.3%. Also, when the distance between group D was 135 mm, the average ultimate bearing capacity increased by approximately 18.0%.

Table 2. Main Bending Test Results

No.	P_u (kN)	ε_c (με)	ε_t (με)	ω (mm)	MOE (MPa)	MOR (MPa)
ZJA1	14.10	-4197	4345	41.95	13643	52.67
ZJA2	14.40	-4045	3778	34.21	12269	53.79
ZJA3	15.06	-3968	4964	47.29	13400	56.23
ZJB1	10.37	-3689	4244	42.93	11345	43.55
ZJB2	10.79	-3802	4085	43.89	12641	45.31
ZJB3	11.10	-3764	3956	42.78	12519	46.61
ZJC1	12.21	-3691	3874	44.16	13126	51.27
ZJC2	12.06	-3834	4155	36.41	13259	50.64
ZJC3	11.94	-3895	4203	41.03	13012	50.14
ZJD1	12.60	-3856	4218	47.68	13939	52.91
ZJD2	13.06	-3975	4534	43.04	13863	54.84
ZJD3	12.40	-3877	4342	43.12	14012	52.07

Notes: ε_c is the ultimate compressive strain at failure (με), ε_t is the tensile strain at failure (με), and ω is the deflection corresponding to the ultimate load (mm).

NUMERICAL ANALYSIS

Unit Selection and Meshing

The solid model of the glulam wood beam was established with a Solid186 solid element. The element was a three-dimensional 20-node high-order hexahedral element with a quadratic displacement mode. Each node had three translational degrees of freedom, and the material nonlinearity and geometric nonlinearity were considered. The finite element model after meshing is shown in Fig. 5.

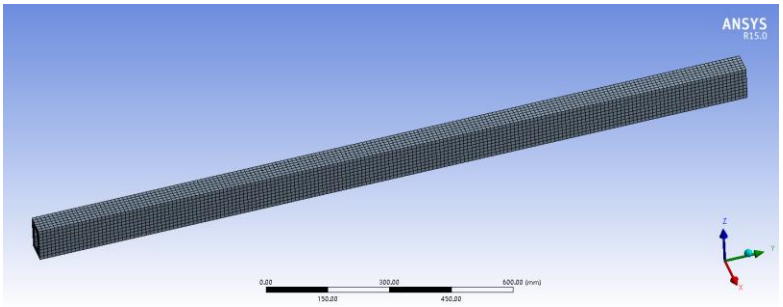

Fig. 5. Finite element model

Material Parameters and Constitutive Model

Wood is an anisotropic material, which means that the establishment of a triaxial constitutive model can be complicated. It has been studied to establish a constitutive model with longitudinal axial mechanical properties. Bechtel and Norris (1952) proposed a bilinear tensile and compressive constitutive model based on many other experiments (Fig. 6). The model assumes that the tension zone is linearly elastic and the compression zone is

also elastic. After the strength reaches the yield, the stress value remains unchanged, which is the ideal elastoplastic model. The mathematical expression of the model is as follows,

$$\sigma = \begin{cases} E\varepsilon, \varepsilon_t \le \varepsilon \le \varepsilon_0 \\ \sigma_0, \varepsilon_0 \le \varepsilon \le \varepsilon_c \end{cases} \quad (3)$$

where E is the flexural modulus of the wood (14016.3 MPa), ε_t is the ultimate tensile strain (5119 με), ε_c is the ultimate compressive strain (5037 με), and σ_0 is the compressive yield strength of the wood (43.05 MPa).

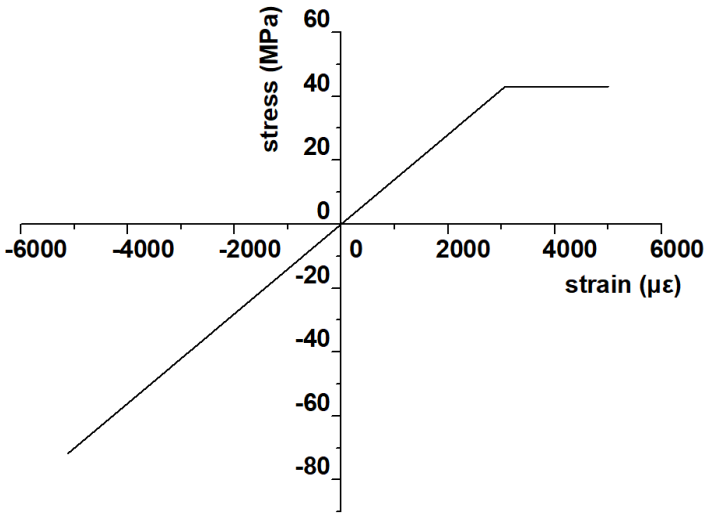

Fig. 6. Stress-strain curve

Loads and Boundary Conditions

The load was applied in the form of a concentrated force, and the loading area was consistent with the size of the loading plate. Consistent with the maintenance boundary condition and the actual test boundary constraint, the pressure-free tension constraint was applied to the bottom portion of the beam end; the constraint area was consistent with the size of the pad. Figure 7 shows the calculation model after applying loads and constraints.

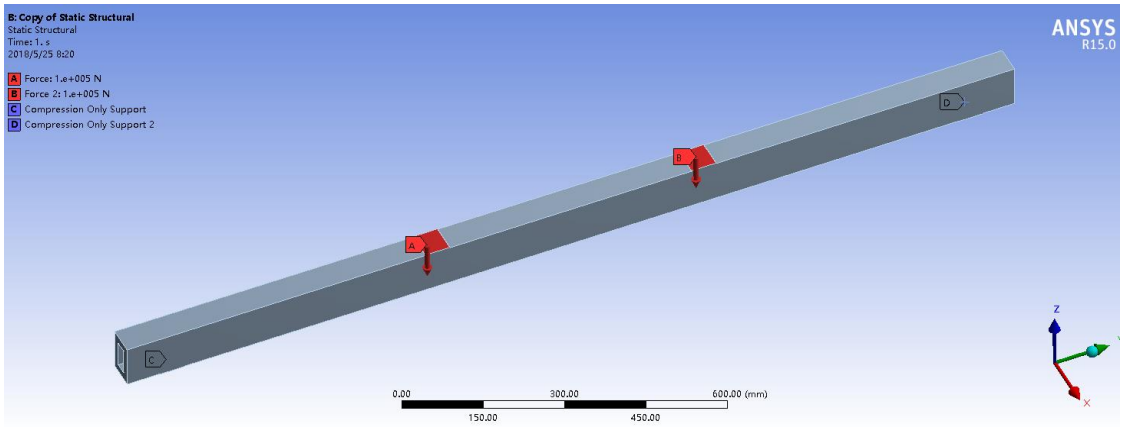

Fig. 7. Loads and constraints of the specimen

Numerical Calculation Results and Analysis

Comparative analysis of the load-deflection curves

The test and numerical analysis results of the load-deflection curves of all of the glulam beam specimens are shown in Fig. 8. Table 3 shows that the finite element numerical calculation had results that agreed with the experiments.

Table 3. Comparison between the Ultimate Load of the Test and FEM

No.	Experiment Average (kN)	Finite Element Analog (kN)	Deviation (%)
ZJA	14.52	15.76	8.5
ZJB	10.75	11.67	8.6
ZJC	12.07	13.00	7.7
ZJD	12.68	14.05	10.8

Because of the finite element simulation analysis, defects, such as knots, were not considered，the MOE and MOR of the numerical analysis curve were therefore slightly higher than those of the test curve. The load displacement curve was divided into three phases. The first stage started from loading to approximately 70% of the ultimate load. In this stage, the deflection curve of the specimen was approximately straight and presented a linear elastic characteristic. The second stage was from the end of the first stage to the ultimate load, and the curve was nonlinear. As the load increased, the wooden beam exhibited a certain degree of plastic bending. At this stage, the hollow beam specimen exhibited better ductility than the solid beam. It can be seen from Table 2 that the ability of the hollow glulam beam to maintain its deformation after its ultimate bearing capacity was better than that of the solid glulam beam. The average deflection of the group B hollow glulam beam specimen was 43.2 mm, and the average deflection value of the group A solid glulam of is 41.15mm. The load-displacement curve in Fig. 8 also intuitively reflected the relationship between the deflections of the two sections under load. The third phase was the failure phase. As the load increased, the stiffness of the timber beam continued to decrease until it was destroyed.

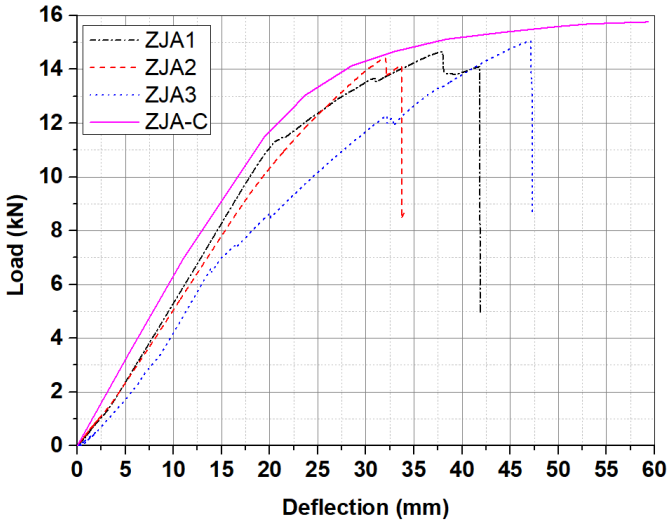

(a)

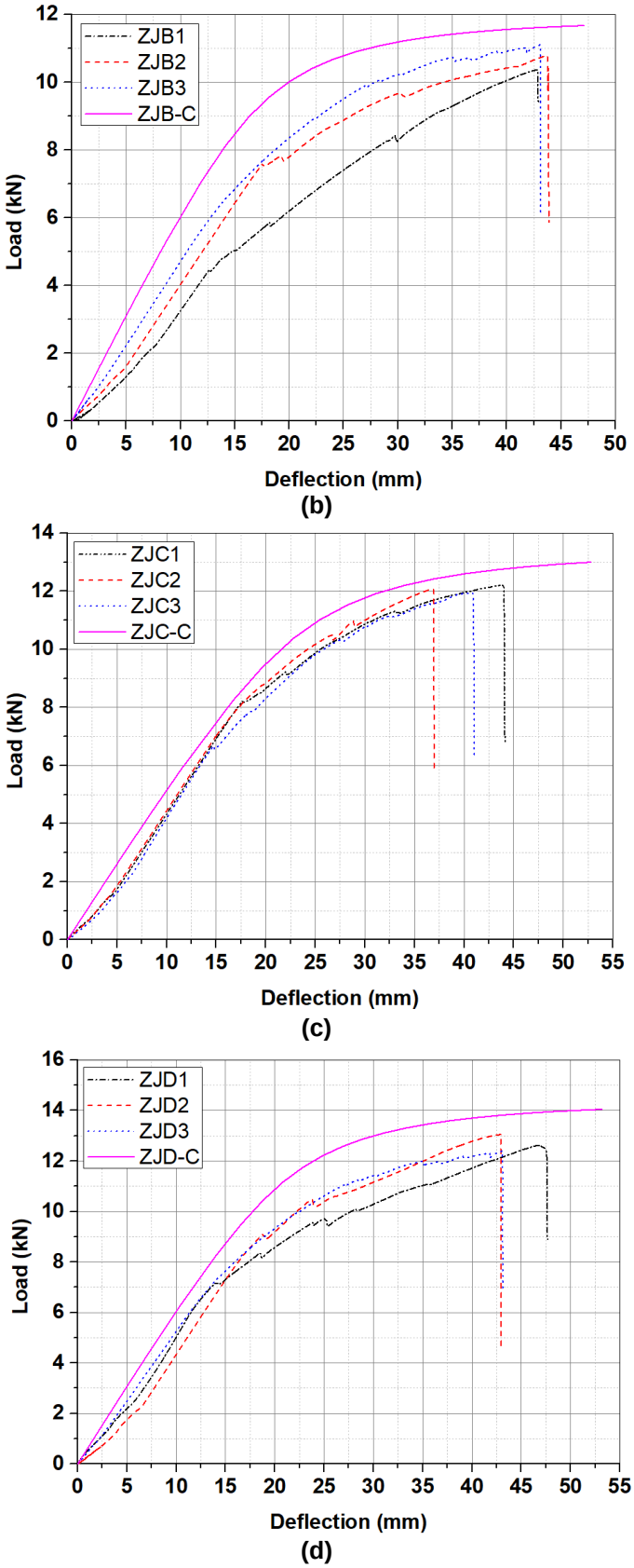

Fig. 8. Load-deflection curve for (a) ZJA, (b) ZJB, (c) ZJC, and (d) ZJD：the denominations of type -C refer to the numerical models

Influence of the stiffener spacing on the ultimate bearing capacity

To determine the optimum stiffener spacing, the relationship between the stiffener spacing and ultimate bearing capacity was obtained using the experimental data and finite element simulation integration. Figure 9 shows that when the ratio of the stiffener rib spacing (*d*) to beam height (*h*) was greater than 3.4, the ultimate bearing capacity changed slightly and the design reference value was of little importance. Therefore, the maximum stiffener spacing was judged to be 3.4*h*. Considering the convenience of hollow beam processing, the recommended spacing is approximately 1.0*h* to 3.4*h*.

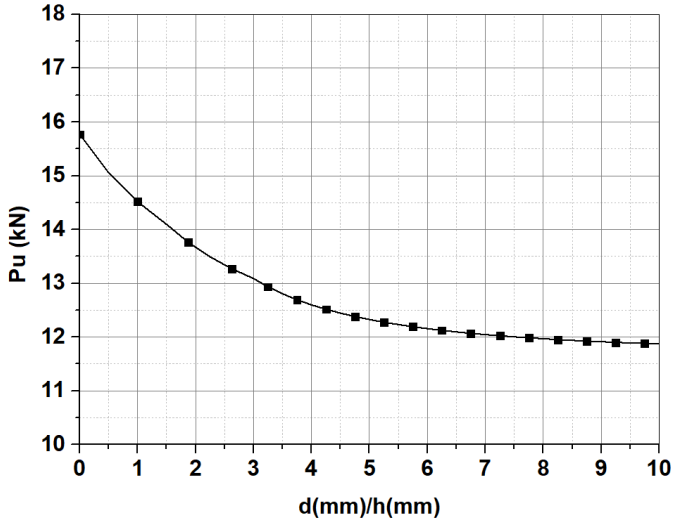

Fig. 9. Graph of the bearing capacity as a function of the stiffener distance

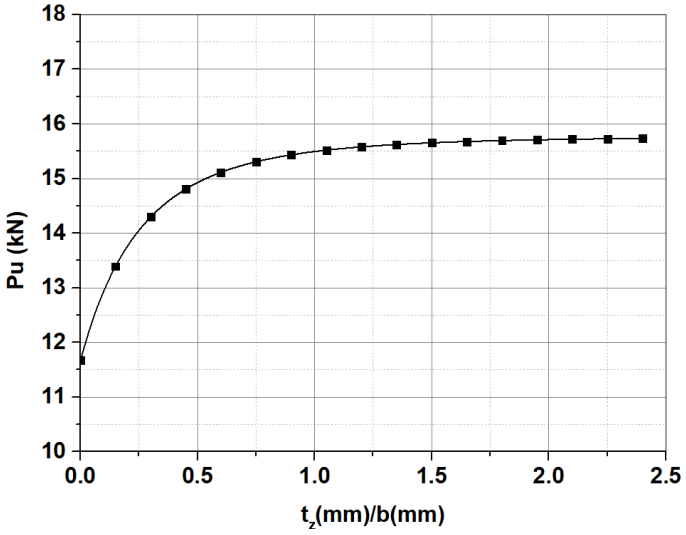

Fig. 10. Graph of the thickness-width ratio of the stiffener and bearing capacity

Effect of the stiffener thickness on the ultimate bearing capacity

To determine the reasonable stiffener thickness, the relationship between the stiffener thickness and ultimate bearing capacity was obtained using the experimental data and finite element simulation integration. Figure 10 shows that when the ratio of the

thickness (t_z) of the stiffener to the width (b) of the beam was greater than 0.5, the ultimate bearing capacity changed slightly and the design reference value was of little importance. Therefore, the maximum thickness of the stiffener was 0.5b. However, considering the structural requirements of the stiffener thickness, the recommended thickness is approximately 0.25b to 0.5b.

CONCLUSIONS

1. The intermittent insertion of glued stiffener pieces improved the ultimate bearing capacity and MOR of the hollow modulus and improved the failure mode of the glulam beam. Compared with the hollow glulam beam, the ultimate bearing capacity was increased by approximately 12.3%, and the ultimate bearing capacity was increased by approximately 18.0% when the spacing was 135 mm. Considering practical applications, the reasonable spacing of the stiffeners was approximately 1.0h to 3.4h and the reasonable thickness of the bamboo-like joints was approximately 0.25b to 0.5b.
2. The wood saving rate of the hollow and bamboo-like glulam beams compared with the solid wood beam was 26.4% and 25.7%, respectively, which not only reduced the self-weight, but also improved the wood utilization rate. Wood is a green renewable resource and combined with the status of domestic timber resources, it is of great importance to make full use of fast-growing, small-diameter Northeast China larch (*L. olgensis* Henry) timber.
3. The numerical analysis results showed agreement with the test results. The load-deflection curve was divided into three stages: linear and nonlinear segments and a failure phase. Because of the presence of defects and different cross-sections of the test specimens, the MOE of the linear segment was 6.51%, 13.18%, 6.30%, and 0.56% smaller than the MOE obtained from the material test, respectively.
4. The continuity and thickness of the adhesive layer had an influence on the mechanical properties of the bamboo-like hollow glulam beam. Therefore, the process parameters, such as the temperature, humidity, sizing quality, thickness of the rubber layer, and curing conditions, should be strictly controlled during production.

ACKNOWLEDGMENTS

The authors are grateful for the support provided by Jiangsu University Students Innovation and Entrepreneurship Project of China (Grant No. 201510298112X), the Natural Science Foundation of China (Grant No. 51808176), and the National Science Foundation of Hainan Province of China (Grant No. 518QN213).

REFERENCES CITED

Adams, R. D., Krueger, G. P., Lund, A. E., and Nicholas, D. D. (1979). "Development of utility poles from composite wood material," in: *Proceedings of the 7th IEEE/PES Transmission and Distribution Conference and Exposition*, Atlanta, GA, pp. 37-40.

Aicher, S., and Tapia, C. (2018). "Novel internally LVL-reinforced glued laminated timber beams with large holes," *Constr. Build. Mater.* 169, 662-677. DOI: 10.1016/j.conbuildmat.2018.02.178

ASTM D4761-13 (2013). "Standard test methods for mechanical properties of lumber and wood-base structural material," American Society for Testing and Materials, West Conshohocken, PA.

ASTM D198-15 (2015). "Standard test methods of static tests of lumber in structural sizes," American Society for Testing and Materials, West Conshohocken, PA.

Anshari, B., Guan, Z., Komatsu, K., Kitamori, A., and Jung, K. (2010). "Explore novel ways to strengthen glulam beams by using compressed Japanese cedar," in: *Proceedings of the World Conference on Timber Engineering (WCTE)*, Riva del Garda, Italy, pp. 8.

Bechtel, S. C., and Norris, C. B. (1952). *Strength of Wood Beam and Rectangular Cross Section as Affected by Span-depth Ratio* (Report No. 1910), U.S. Department of Agriculture Forest Products Laboratory, Madison, WI

Bradford, M. A., Hassanieh, A., Valipour, H. R., and Foster, S. J. (2017). "Sustainable steel-timber joints for framed structures," *Procedia Engineer.* 172, 2-12. DOI: 10.1016/j.proeng.2017.02.011

Cai, X. R. (2014). *Study on Structural Processes and Performance of Laminated Veneer Hollow Column*, Master's Thesis, Nanjing Forestry University, Nanjing, China.

Capozucca, R. (1998). "Bond stress system of composite concrete-timber beams," *Mater. Struct.* 31(9), 634-640. DOI: 10.1007/BF02480615

CECS 254 (2009). "Technical specification of hollow concrete-filled steel tubular structures," China Association for Engineering Construction Standardization, Beijing, China.

Eisenhut, L., Seim, W., and Kühlborn, S. (2016). "Adhesive-bonded timber-concrete composites – Experimental and numerical investigation of hygrothermal effects," *Eng. Struct.* 125, 167-178. DOI: 10.1016/j.engstruct.2016.05.056

GB 50005 (2003). "Code for design of timber structures," Ministry of Housing and Urban Rural Development of the People's Republic of China Press, Beijing, China.

GB/T 50329 (2012). "Standard for test methods of timber structures," Standardization Administration of China, Beijing, China.

Ghavami, K. (1995). "Ultimate load behavior of bamboo-reinforced lightweight concrete beams," *Cement Concrete Comp.* 17(4), 281-288. DOI: 10.1016/0958-9465(95)00018-8

Gilbert, B. P., Underhill, I. D., Bailleres, H., El Hanandeh, A., and McGavin, R. L. (2014). "Veneer based composite hollow utility poles manufactured from hardwood plantation thinned trees," *Constr. Build. Mater.* 66, 458-466. DOI: 10.1016/j.conbuildmat.2014.05.093

Gilbert, B. P., Underhill, I. D., Fernando, D., Bailleres, H., and Miller, D. (2018). "Structural behaviour of hardwood veneer-based circular hollow sections of different compactness," *Constr. Build. Mater.* 170, 557-569. DOI: 10.1016/j.conbuildmat.2018.03.105

Hara, Y., Kawai, S., and Sasaki, H. (1994). "Manufacture and mechanical properties of cylindrical laminated veneer lumber," *Wood Research: Bulletin of the Wood Research Institute Kyoto University* 81, 28-30.

Harries, K. A., Petrou, M. F., and Brooks, G. (2000). "Structural characterization of built-up timber columns," *Journal of Architectural Engineering* 6(2), 58-65. DOI: 10.1061/(ASCE)1076-0431(2000)6:2(58)

Hartig, J. U., Wehsener, J., and Haller, P. (2016). "Experimental and theoretical investigations on moulded wooden tubes made of beech (*Fagus sylvatica* L.)," *Constr. Build. Mater.* 126, 527-536. DOI: 10.1016/j.conbuildmat.2016.09.042

Keipour, N., Valipour, H. R., and Bradford, M. A. (2018). "Experimental study of steel-timber composite (STC) beam to steel column joints having a flush end-plate," *Eng. Struct.* 174, 906-918. DOI: 10.1016/j.engstruct.2018.08.009

Sasaki, H., and Kawai, S. (1994). "Recent research and development work on wood composites in Japan," *Wood Sci. Technol.* 28(4), 241-248. DOI: 10.1007/BF00204210

Shang, P., Sun, Y., Zhou, D., Qin, K., and Yang, X. (2018). "Experimental study of the bending performance of hollow glulam beams," *Wood Fiber Sci.* 50(1), 3-19.

Wang, J.-l., Jin, H.-x., Yang, Z.-b., and Wang, G. (2008). "Species diversity and productivity of *Larix principis-rupprechtii* plantation woods in Liupan mountains," *Journal of Lanzhou University (Natural Sciences)* 44(1), 31-42.

Wei, Y.-x. (2005). *Study on Properties of Glass Fiber Reinforced Cylindrical Veneer Lumber*, Master's Thesis, Northeast Forestry University, Harbin, China.

Zhang, Q., Zhu, Y.-x., Jiang, S., Wen, S., and Zhang, X. (1997). "Preliminary study on bamboo-wood composite hollow slab for structure," *China Forest Products Industry* 3, 4-6. DOI: 10.19531/j.issn1001-5299.1997.03.003

Zhao, Q., Chen, C., and Pan, J. (2014). "Experimental study on bending behavior of wooden beams with upper and lower joints," *Industrial Construction* 44(8), 103-107. DOI: 10.13204/j.gyjz201408022

Article submitted: October 30, 2018; Peer review completed: January 1, 2019; Revised version received and accepted: January 22, 2019; Published: January 30, 2019.
DOI: 10.15376/biores.14.1.2171-2185